



Simple Method for Fabrication of Three-Dimensional (3D) Copper Nanostructured Architecture by Electrodeposition

Susumu Arai*^z and Tomoya Kitamura

Departments of Chemistry and Material Engineering, Faculty of Engineering, Shinshu University, Nagano-shi, Nagano 380-8553, Japan

Three-dimensional (3D) copper nanostructured architectures were fabricated on a copper substrate using a simple electrodeposition technique. An acid copper sulfate bath was used for copper plating with polyacrylic acid (PA) as an additive and electrodeposition was performed under galvanostatic conditions. The surface morphology of the electrodeposited copper films was significantly changed and a 3D nanostructured architecture that consisted of highly porous 50 nm thick sheet-like copper deposits was obtained by the addition of PA. It is considered that such a 3D nanostructured architecture could be applied as a current collector for lithium-ion battery anodes.

© 2014 The Electrochemical Society. [DOI: 10.1149/2.004405eel] All rights reserved.

Manuscript submitted February 10, 2014; revised manuscript received February 27, 2014. Published March 12, 2014.

Three-dimensional (3D) nanostructured architectures have been developed for functional devices such as supercapacitors,¹ fuel cells,² and batteries³ because of their superior potential for rapid electrochemical reactions due to large specific surface areas. 3D copper nanostructured architectures are particularly attractive for use with electrode materials and there have been vigorous efforts to develop suitable fabrication techniques. Fibrous copper nanostructured electrodes for CO₂ electroreduction have been formed using a procedure that combines high-temperature annealing and electroreduction.⁴ Nanoporous copper for tin based lithium ion battery anodes was fabricated by de-alloying aluminum from an Al-Cu alloy.⁵ To fabricate 3D copper nanostructures for lithium ion battery electrodes, nanoporous copper structures^{6,7} for tin based anodes⁸ were formed by electrodeposition using hydrogen bubbles as a template, and a copper nanopillar current collector for Sn-Ni based anodes was formed by electrodeposition through a porous alumina membrane.⁹

Although these 3D copper nanostructured architectures are very effective for improving electrode functions, many steps are required during fabrication. Therefore, a very simple electrodeposition method is investigated here for fabricating 3D copper nanostructured architectures, where an organic additive is added to the electrodeposition bath.

Experimental

An acidic copper sulfate bath (0.85 M CuSO₄ · 5H₂O + 0.55 M H₂SO₄) was used as the base plating bath and polyacrylic acid (mean molecular weight 5000; PA-5000) was used as an additive. Electrodeposition was conducted under galvanostatic conditions (1 A dm⁻²) without agitation at 25 °C. A pure copper plate (JIS C1201P) with an exposed surface area of 10 cm² (3.3 × 3 cm²) was used as the substrate. A copper plate containing phosphorus was used as the anode. A commercially available electrolytic cell (Model I, Yamamoto-Ms Co. Ltd) with internal dimensions of 65 × 65 × 95 mm³ was employed for electrodeposition, where the volume of the plating bath was 250 cm³.

The surface and cross-sectional morphologies of the copper films were examined using field emission-scanning electron microscopy (FE-SEM; SU-8000, Hitachi). A cross-section polisher (SM-09010, JEOL) was used to prepare cross-sectional samples for FE-SEM observation. The phase structures of the copper films were examined using X-ray diffraction (XRD; XRD-6000, Shimadzu Seisakusho). Thick copper films were electrodeposited (54 C cm⁻², ca. 20 μm thick dense copper film) on copper substrates for XRD measurements to avoid the influence of the copper substrate.

Cathode polarization measurements were conducted using an electrochemical measurement system (HZ-5000, Hokuto Denko) to clarify

the effects of PA-5000 on the electrodeposition of copper. A pure copper plate, platinum plate, and a saturated calomel electrode (SCE) were used as the working, counter, and reference electrodes, respectively. Measurements were performed without agitation at 25 °C.

Results and Discussion

Figure 1 shows surface and cross-sectional SEM images of copper films electrodeposited with various PA-5000 concentrations. The white dotted lines shown in Figs. 1d–1f indicate the boundaries of the copper substrates and electrodeposited copper films. The amount of charge used for all samples was 2.7 C cm⁻², which corresponds to 1 μm thick film deposition if the current efficiency is 100%. Figure 1a shows the surface morphology of a copper film electrodeposited from a plating bath without PA-5000. Electrodeposited copper grains with diameters of ca. 1 μm were observed and the surface was rough. Figure 1d shows the cross-sectional morphology of the surface in Fig. 1a; the copper film is dense and free of voids and is approximately 1 μm thick. In contrast, the surface and cross-sectional morphologies were changed with PA-5000 concentrations in the range of 1–5 × 10⁻⁴ M, and especially in the range of 2–3 × 10⁻⁴ M (Figs. 1b, 1e). The copper film in Fig. 1b consists of thin sheet-like copper deposits and the surface is very rough. The total thickness of the film is ca. 4 μm and it contains many voids (Fig. 1e). As the current efficiency of this copper film was ca. 100%, the porosity of this film was estimated from the film thickness to be ca. 75%; therefore, this copper film has a 3D nanostructured architecture. The surface morphology becomes smooth when the PA-5000 concentration exceeds 1 × 10⁻³ M (Fig. 1c) and the film is dense (Fig. 1f). Therefore, the copper 3D nanostructured architecture can be controlled according to the PA-5000 concentration.

Figure 2 shows surface SEM images of copper films electrodeposited from a plating bath containing PA-5000 (3 × 10⁻⁴ M) using various amounts of charge. Growth of the sheet-like copper deposits increased with the amount of charge, accompanied by an increase of surface roughness. Although the sheet-like copper deposits grew in the horizontal direction, there was little growth in the vertical direction, so that the film thickness remained almost constant, despite an increase in the amount of charge. The thickness of the copper deposits was estimated to be ca. 50 nm from Figs. 2a–2c. Thus, the surface roughness of the 3D copper nanostructured architectures can be changed according to the amount of charge used. Regarding the adhesion and robustness of the 3D copper nanostructure, the sheet-like copper deposits were not exfoliated from the copper substrate or deformed by running water during the rinsing process. Therefore, the 3D copper nanostructure is considered to have sufficient adhesive properties and robustness.

Figure 3 shows XRD patterns for copper films electrodeposited in plating baths with various PA-5000 concentrations. The copper film electrodeposited from the base plating bath without PA-5000

*Electrochemical Society Active Member.

^zE-mail: araisun@shinshu-u.ac.jp

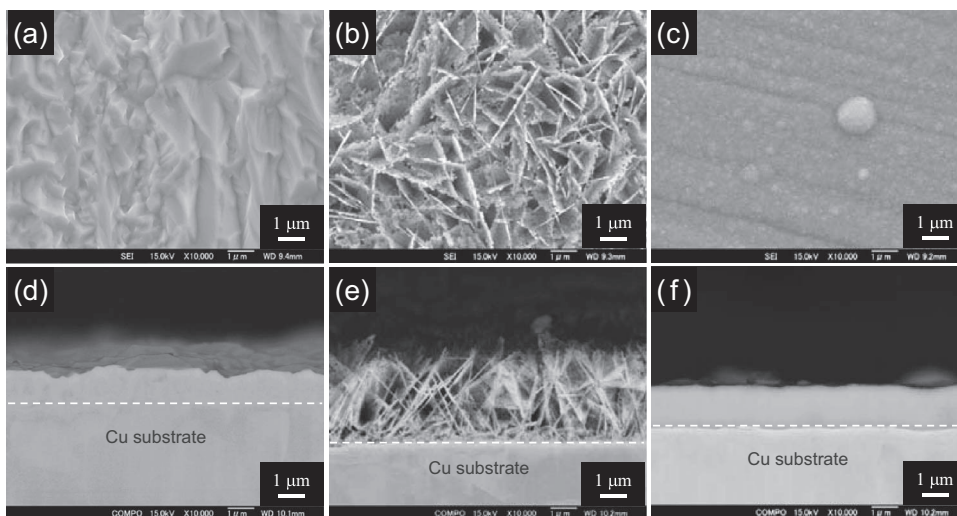


Figure 1. Surface and cross-sectional SEM images of copper films. Surface SEM images of copper films electrodeposited with PA-5000 concentrations of (a) 0, (b) 3×10^{-4} , and (c) 2×10^{-3} M. (d)-(f) Cross-sectional SEM images of (a)-(c), respectively. The amount of charge used was 2.7 C cm^{-2} . The white dashed lines in (d)-(f) indicate the boundary of the copper substrate and electrodeposited copper film.

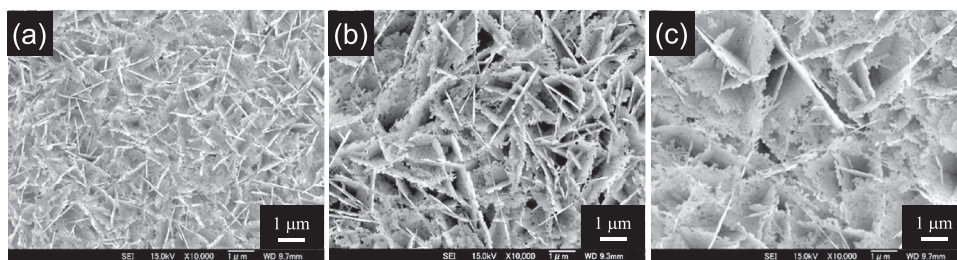


Figure 2. Surface SEM images of copper films electrodeposited with various amounts of charge; (a) 14 C, (b) 27 C, and 54 C. The PA-5000 concentration used was 3×10^{-4} M.

(Fig. 3a) had diffraction peaks that were all assigned to face-centered cubic copper. Sharp diffraction peaks were observed for the film electrodeposited with a PA-5000 concentration of ca. 2×10^{-4} M (Fig. 3c), which indicates high crystallinity. In contrast, a broad diffraction peak was observed for the film deposited with a PA-5000 concentration of 2×10^{-3} M (Fig. 3d), which indicates low crystallinity and possibly an amorphous structure. The copper film electrodeposited from the plating bath with 2×10^{-4} M PA-5000 has a 3D nanostructured architecture and a high degree of crystallinity; therefore, the conductivity of this film is expected to be similar to that of pure copper.

Figure 4 shows the shift in the cathode polarization curves for the copper plating baths toward the negative side with increasing PA-5000 concentration. PA-5000 should not form a complex ion with the Cu^{2+} ion in a strong acid, such as the acidic copper sulfate bath used in this study; therefore, it is considered that PA-5000 is adsorbed onto the copper film surfaces during electrodeposition, which inhibits the electrodeposition of copper. The formation of unique 3D copper nanostructured architectures is thus considered to be related to the adsorption of PA-5000 onto the copper film.

Figure 5 shows the proposed mechanism for the growth of the 3D copper nanostructured architectures. Prior to application of the voltage, PA-5000 is adsorbed onto the cathode (Cu substrate) surface (Fig. 5a). When the voltage is applied, copper nuclei are electrodeposited onto the copper substrate. Subsequently, the electrodeposi-

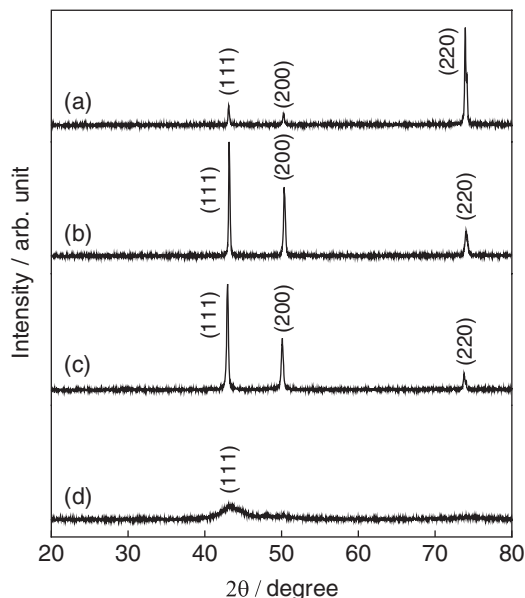


Figure 3. XRD patterns for copper films electrodeposited with various PA-5000 concentrations; (a) 0, (b) 2×10^{-5} , (c) 2×10^{-4} , and 2×10^{-3} M.

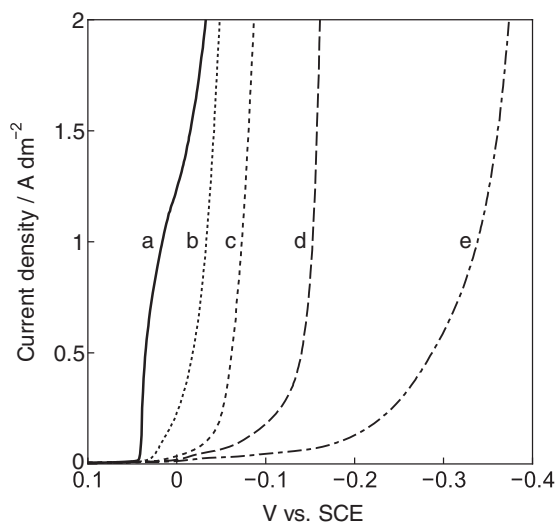


Figure 4. Cathodic polarization curves for copper plating baths containing PA-5000 at concentrations of (a) 0, (b) 2×10^{-6} , (c) 2×10^{-5} , (d) 2×10^{-4} , and (e) 2×10^{-3} M.

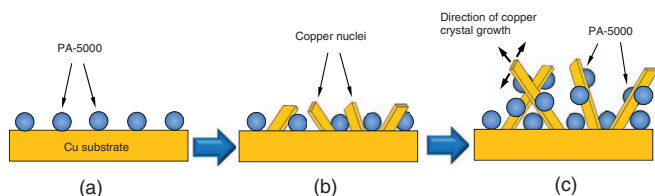


Figure 5. Proposed mechanism for the growth of 3D copper nanostructured architectures. (a) Before electrodeposition, PA-5000 adsorbs onto the copper substrate. (b) At the early stage of electrodeposition; copper nuclei are formed on the copper substrate. (c) During electrodeposition; PA-5000 adsorbs onto specific crystal plane(s) of the copper deposits and copper crystal growth occurs only on limited crystal plane(s) to form a 3D copper nanostructured architecture that consists of sheet-like copper deposits.

tion of copper continues under galvanostatic conditions. In the case of PA-5000 concentrations of $1-5 \times 10^{-4}$ M and especially at $2-3 \times 10^{-4}$ M, PA-5000 may adsorb onto specific crystal plane(s) of the copper deposits and inhibit the crystal growth of copper on these specific crystal plane(s). Copper should then grow only on the other crystal plane(s), which results in sheet-like copper deposits with a 3D nanostructured architecture (Fig. 5c). The order of the surface free energy of each crystal plane $\gamma_{(hkl)}$, for metals having face-centered cubic crystal structures, such as copper, is generally $\gamma_{(111)} < \gamma_{(100)} < \gamma_{(110)}$ at room temperature, according to the broken-bond model.¹⁰ Therefore, if PA-5000 is selectively adsorbed onto the most unstable copper crystal planes, i.e., the (220) planes ((110) planes) of electrodeposited copper, then the resulting selective copper crystal growth will occur on other crystal planes, such as the (200) planes ((100) planes). Future work will include a detailed investigation of the copper crystal growth mechanism.

Conclusions

The effect of PA-5000 addition to an acidic copper sulfate electrodeposition bath was investigated for the fabrication of 3D copper nanostructured architectures. A 3D copper nanostructured architecture that consists of sheet-like copper deposits with a thickness of ca. 50 nm and relatively high porosity was fabricated by the addition of PA-5000. Such 3D copper nanostructured architectures may be useful for application to functional electrodes, such as a current collector material for lithium-ion battery anodes.

References

1. S. Ghosh and O. Inganäs, *Adv. Mater.*, **11**, 1214 (1999).
2. Y. Liu, S. Zha, and M. Liu, *Adv. Mater.*, **16**, 256 (2004).
3. D. R. Rolison and B. Dunn, *J. Mater. Chem.*, **11**, 963 (2001).
4. J. Qiao, P. Jiang, J. Liu, and J. Zhang, *Electrochem. Commun.*, **38**, 8 (2014).
5. S. Zhang, Y. Xing, T. Jiang, Z. Du, F. Li, L. He, and W. Liu, *J. Power Sources*, **196**, 6915 (2011).
6. H. C. Shin, J. Dong, and M. Liu, *Adv. Mater.*, **15**, 1610 (2003).
7. H. C. Shin and M. Liu, *Chem. Mater.*, **16**, 5460 (2004).
8. T. Jiang, S. Zhang, X. Qiu, W. Zhu, and L. Chen, *J. Power Sources*, **166**, 503 (2007).
9. J. Hassoun, S. Panero, P. Simon, P. L. Taberna, and B. Scrosati, *Adv. Mater.*, **19**, 1632 (2007).
10. J. K. Mackenzie, A. J. W. Moore, and J. F. Nicholas, *J. Phys. Chem. Solids*, **23**, 185 (1962).